

## Supporting Information

# Turn-On Solid State Luminescence by Solvent-Induced Modification of Intermolecular Interactions

*Prabhat Majumdar,<sup>a</sup> Madhubrata Ghora,<sup>a</sup> Reinhold Wannemacher,<sup>b</sup> Johannes Gierschner<sup>b</sup>  
and Shinto Varghese<sup>\*a</sup>*

<sup>a</sup> Technical Research Centre & School of Applied and Interdisciplinary Sciences, Indian  
Association for the Cultivation of Science, Kolkata-700032, India

<sup>b</sup> Madrid Institute for Advanced Studies, IMDEA Nanoscience, C/Faraday 9, Ciudad  
Universitaria de Cantoblanco 28049, Madrid, Spain.

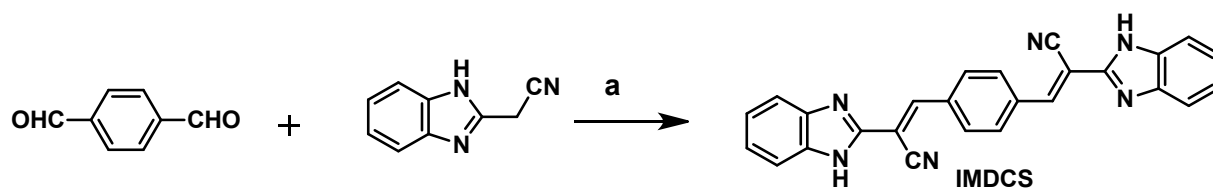
\* E-mail: [Shinto.Varghese@iacs.res.in](mailto:Shinto.Varghese@iacs.res.in)

Table of Contents		Page No.
1.	Materials and Instrumentation	3
2.	Synthesis and Characterization	4
3.	<b>Figure S1.</b> The dimer arrangement in the crystal lattice of the Y-form	4
4.	<b>Table S2.</b> Summary of Crystallographic Data for IMDCS.	5
5.	<b>Figure S3.</b> a) The finger print plot and the b) percentage contribution of the intermolecular interactions.	5
6.	<b>Figure S4.</b> The interaction energy of the nearest neighbours of the IMDCS.	6
7.	<b>Figure S5.</b> Differential scanning calorimetric analysis (DSC) of different forms of IMDCS	6
8.	<b>Figure S6.</b> Thermogravimetric analysis (TGA) of different forms of IMDCS	6
9.	<b>Figure S7.</b> Photophysical properties in solution; <b>a)</b> Absorption and emission spectra <b>b)</b> fluorescence decay traces in solution.	7
10.	<b>Figure S8.</b> The gradual shift of emission spectra from 550 nm to 625 nm of the Y-form on exposure to methanol vapours and the recovery on addition of DMSO.	7
11.	<b>Table S9.</b> Photophysical characterization of IMDCS chromophore in solution and solid state.	8
12.	<b>Table S10.</b> The calculated vertical transition energies of IMDCS in solution at TD-DFT level of theory (PCM/CAM-B3LYP/6-31G(d,p)).	8
13.	Description of QM:MM calculations	9
14.	<b>Table S11.</b> The vertical transition energies of IMDCS in Y-form.	9

## 1. Materials and Instrumentation

All chemicals were obtained from commercial suppliers and used as received without further purification.  $^1\text{H-NMR}$  spectra were recorded on a **Bruker DPX** 400 MHz spectrometer using DMSO- $d_6$  as the solvent. High Resolution Mass Spectra (HRMS) were measured in a Micromass Q-TOF micro mass spectrometer with a Z-spray ion source. IR spectra were recorded in Perkin-Elmer Spectrum-100 FT-IR spectrometer. UV/Vis studies were done in a Jasco V-750 spectrometer. Fluorescence spectra were recorded in a Horiba FluoroMax3 spectrometer. Fluorescence quantum yields, with an estimated reproducibility of around 10%, were determined by comparison with Coumarin 153 Dye in ethanol ( $\Phi_F = 0.38$ ), which was used as the fluorescence standard. The absolute fluorescence  $\Phi_F$  values in solid state were determined in an integrating sphere setup (Hamamatsu C9920) equipped with a xenon high-pressure lamp. Fluorescence lifetimes were measured using IBH (FluoroCube) Time-Correlated Picosecond Single Photon Counting (TCSPC) system. Samples were excited with a pulsed diode laser (<100 ps pulse duration) at a wavelength of 375 nm (NanoLED-11) with a repetition rate of 1 MHz. The detection system consisted of a micro channel plate photomultiplier (5000U-09B, Hamamatsu) with a 38.6 ps response time coupled to a monochromator (5000M) and TCSPC electronics (Data station Hub including Hub-NL, NanoLED controller and preinstalled Fluorescence Measurement and Analysis Studio (FMAS) Software). The fluorescence lifetime values were obtained using DAS6 decay analysis software. X-ray single crystal data of the single crystals were collected at low temperature (120-150 K) using Mo  $K\alpha$  ( $\lambda = 0.7107 \text{ \AA}$ ) radiation on a Bruker D8 VENTURE with  $1\mu\text{S}$  3.0 microfocus X-ray source and a CMOS detector. Data collection was carried out using the software package of APEX III. Data reduction and refinements were performed using ShelXL and Olex2 1.2. For visualization of the crystal structures MERCURY (CSD software), Chemcraft and ChemBio 3D ultra 11 were used. Powder XRD was performed on Rigaku SmartLab X-Ray diffractometer using Cu cathode, 40 keV- 110 mA power with Ni filter equipped with 1-D detector. DSC of the samples was done on DSC-Q2000 by TA instruments with heating rate of  $10^\circ \text{ min}^{-1}$  under nitrogen atmosphere. TGA analysis was carried out in a NETZSCH STA 449F3 at a rate of  $20^\circ \text{ C/min}$ . SEM analysis was done in JEOL JSM 6700F. Theoretical calculations were carried out in Gaussian 16, Revision B.01 program. NCI analysis was carried out in the Multiwfn 3.7 software, visualized in VMD and plotted using GNU plot.

## 2. Synthesis and Characterization.



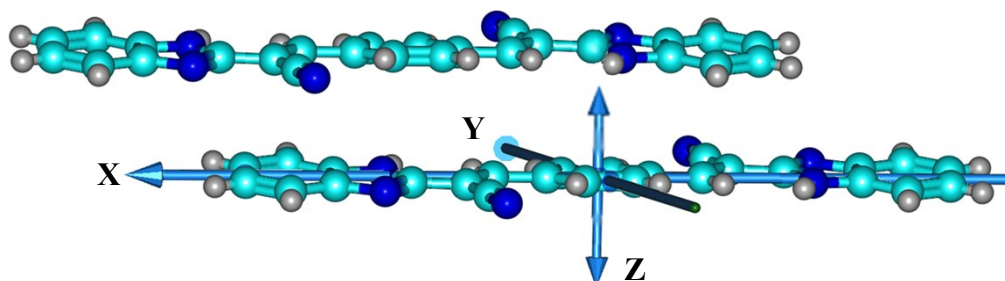
**Scheme S1.** Reagents and Conditions: a) Piperidine (0.2 ml), EtOH reflux, 5 h.

To a stirred solution of Terephthalaldehyde (200 mg, 1.49 mmol) and 2-benzimidazolylacetonitrile (491 mg, 3.13 mmol) in ethanol, piperidine (0.2 ml) was added and refluxed for five hours to get a red precipitate. The precipitate was filtered and then washed with water and subsequently with methanol.

IMDCS: Yield: 467 mg, 76% ; m.p.: Decomp < 300°C ; IR  $\nu_{\max}$  (KBr): 3318, 3058, 3054, 2920, 2237, 1631, 1605, 1436, 1420, 1373, 1315, 1278, 1251, 1230, 1146, 1120, 956, 914, 840, 819, 771, 750, 629, 586, 512, 439  $\text{cm}^{-1}$ ;  $^1\text{H}$  NMR (400 MHz, DMSO- $d_6$ ) :  $\delta$  13.2 (s, 2H), 8.42 (s, 2H), 8.19 (s, 4H), 7.73 (d,  $J = 8$  Hz, 2H), 7.59 (d,  $J = 7.6$  Hz, 2H), 7.26 (m, 4H);  $^{13}\text{C}$  NMR (100 MHz, DMSO- $d_6$ ):  $\delta$  147.08, 143.7, 135.1, 130.0, 123.9, 115.9, 103.8 ppm.

Exact mass calculated for  $\text{C}_{26}\text{H}_{16}\text{N}_6$  ( $\text{M}^+$ ) 413.15; found 413.18 HRMS (TOF MS ES+);  $\text{C}_{26}\text{H}_{16}\text{N}_6$ : calcd C, 75.71; H, 3.91; N, 20.38; found: C, 76.01; H, 3.91; N, 20.29.

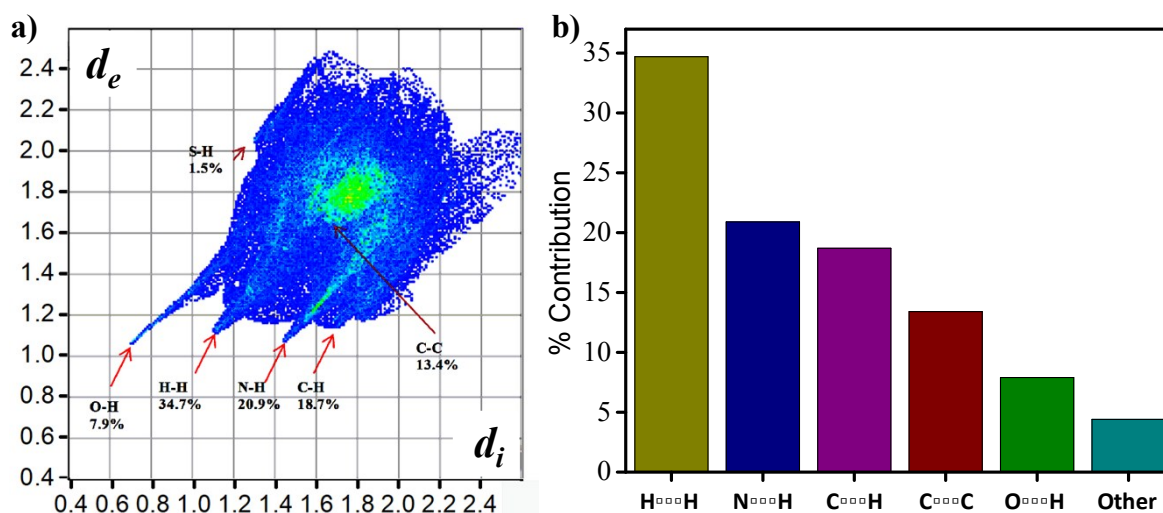
**Note** : IMDCS can also be synthesized in an acidic condition in good yield (74%) by using sodium acetate as reagent in glacial acetic acid. Sodium acetate (610 mg, 7.45 mmol) was dissolved in glacial acetic acid and was heated to 50 °C. Terephthalaldehyde (200 mg, 1.49 mmol) was then added and stirred until a clear homogenous solution was obtained. To this 2-benzimidazolylacetonitrile (491 mg, 3.13 mmol) was added which results in the instantaneous formation of orange/red precipitate. The reaction mixture was stirred for 10 minutes and poured into water, filtered and washed with methanol.



**Figure S1.** The dimer arrangement in the crystal lattice of the Y-form with a long axis slip ( $\Delta x = 5.33 \text{ \AA}$ ), short axis slip ( $\Delta y = 0.14 \text{ \AA}$ ) and  $\pi$ - $\pi$  stacking distance of ( $\Delta z = 3.33 \text{ \AA}$ ).

**Table S2.** Summary of Crystallographic Data for IMDCS Y-form

Empirical formula	C <sub>30</sub> H <sub>28</sub> N <sub>6</sub> O <sub>2</sub> S <sub>2</sub>
Formula weight	568.7
Temperature/K	120.17
Crystal system	triclinic
Space group	P-1
a/Å, b/Å, c/Å	6.260(2), 10.266(3), 12.266(4)
α/°, β/°, γ/°	111.862(10), 95.559(11), 100.950(10)
Volume/Å <sup>3</sup>	705.9(4)
Z	1
ρ <sub>calc</sub> /cm <sup>3</sup>	1.338
μ/mm <sup>-1</sup>	0.228
F(000)	298
Crystal size/mm <sup>3</sup>	0.28 × 0.09 × 0.05
Radiation	MoKα (λ = 0.71073)
2θ range for data collection/°	6.746 to 49.998
Index ranges	-7 ≤ h ≤ 7, -11 ≤ k ≤ 12, -14 ≤ l ≤ 14
Reflections collected	5832
Independent reflections	2466 [R <sub>int</sub> = 0.0670, R <sub>sigma</sub> = 0.0841]
Data/restraints/parameters	2466/0/183
Goodness-of-fit on F <sup>2</sup>	1.054
Final R indexes [I ≥ 2σ (I)]	R <sub>1</sub> = 0.0694, wR <sub>2</sub> = 0.1935
Final R indexes [all data]	R <sub>1</sub> = 0.0813, wR <sub>2</sub> = 0.2050
Largest diff. peak/hole / e Å <sup>-3</sup>	0.72/-0.54
R-Factor (%)	6.90

**Figure S3.** a) The finger print plot and the b) percentage contribution of the intermolecular interactions that stabilize the molecular packing in the crystal lattice of the Y-form.

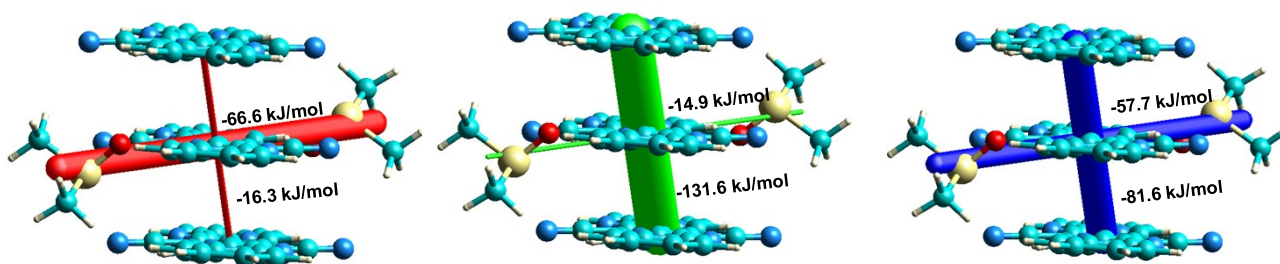


**Figure S4.** The interaction energy of the nearest neighbours of the IMDCS having major contributions (electrostatic-Red, Dispersion-Green and Total energy-blue). The total interaction energy is sum of the model electrostatic, dispersion, polarization and exchange-repulsion terms. The values represented are in kJ/mol.

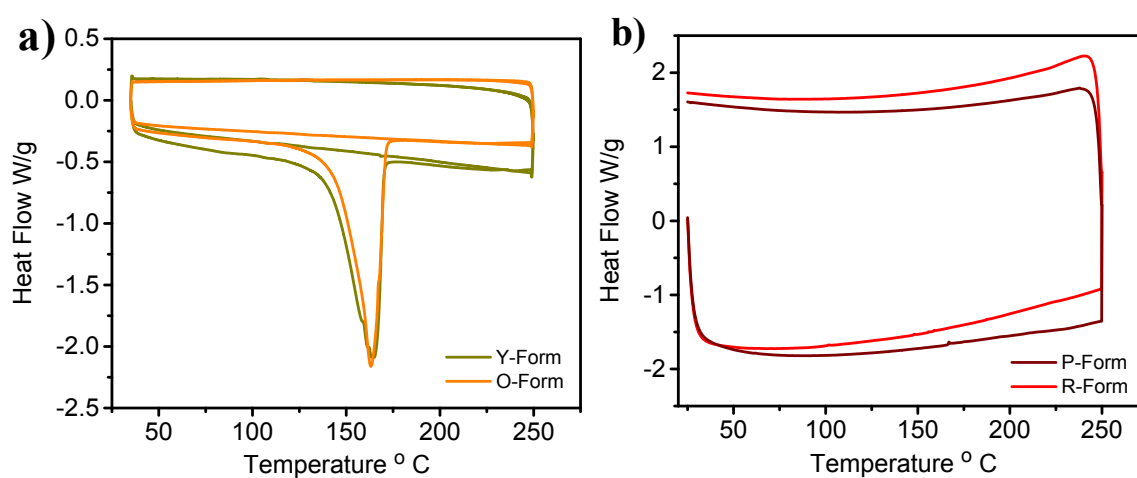


**Figure S5** a) Differential scanning calorimetry (DSC) thermograms of IMDCS a) Y- and O-forms (First and second cycles), b) Pristine and R-form with methanol exposure.

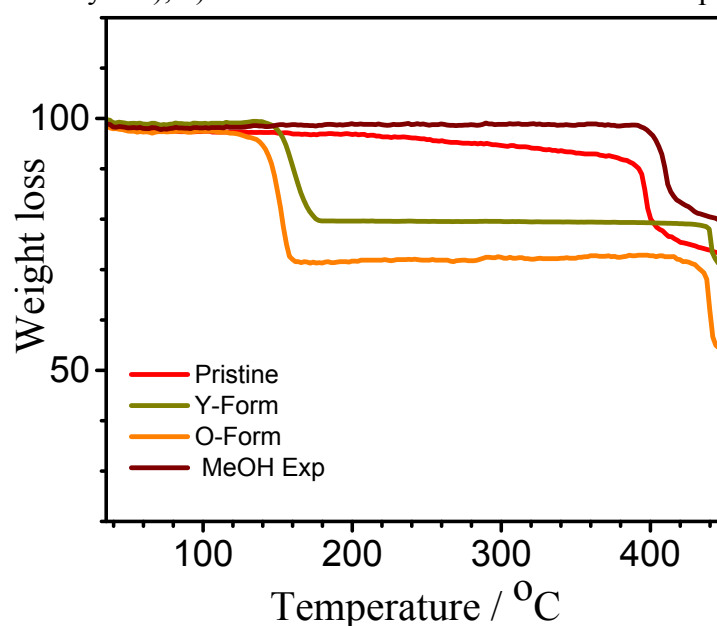


**Figure S6.** Thermogravimetric analysis of different forms of IMDCS. A Weight loss of 20% and 28% at around 160 °C was observed for Y- and O-forms respectively.

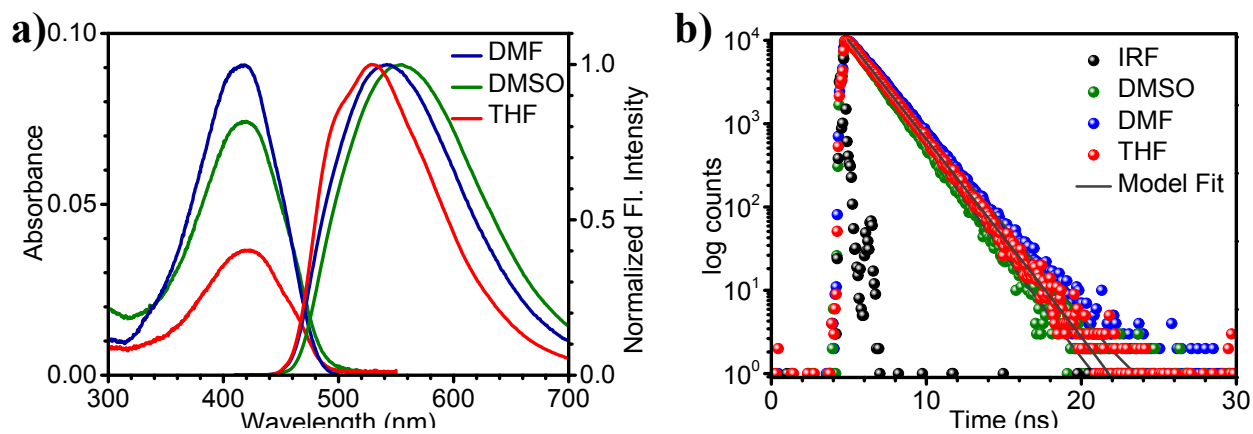


**Figure S7.** Photophysical properties in solution; **a)** Absorption and emission spectra **b)** fluorescence decay traces in solution.

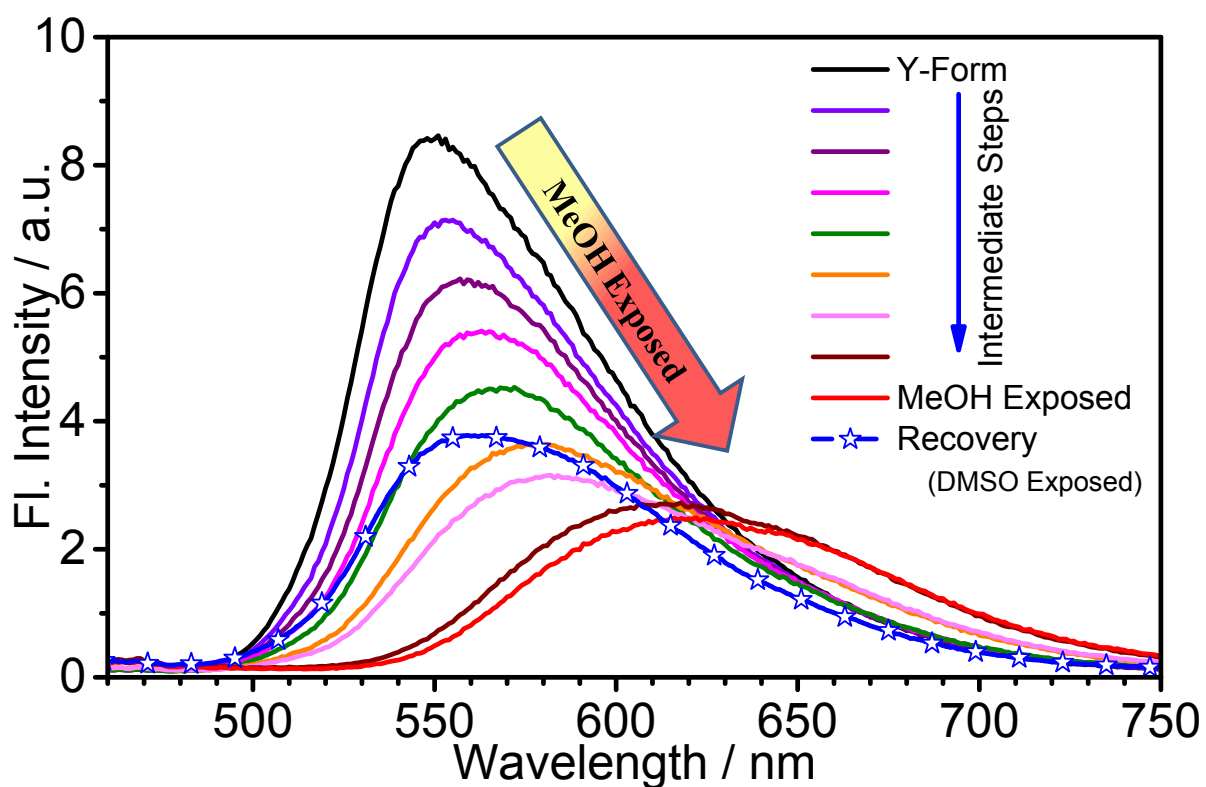


**Figure S8.** The gradual shift of emission maxima from 550 nm to 625 nm of the Y-form on exposure to methanol vapours and recovery on DMSO addition.

**Table S9.** Photophysical characterization of IMDCS chromophore in solution and solid state.

IMDCS	$\lambda_F$ (nm)	$\phi_F$	$\tau_F$ (ns) / (%)	$\langle\tau_F\rangle$ / (ns)	$k_r$ [ns <sup>-1</sup> ]	$k_{nr}$ [ns <sup>-1</sup> ]
THF	529	0.37	1.84 (100)	-	0.20	0.34
DMF	543	0.40	1.95 (100)	-	0.21	0.31
DMSO	556	0.34	1.69 (100)	-	0.20	0.39
Y-form	555	0.37	0.33 (15.83), 0.92 (67.06), 2.32 (17.11)	1.41	0.26	0.45
O-form	588	0.04	1.70 (11.90), 6.35(88.10)	6.19	0.006	0.155
Pristine	623	0.01	1.09 (59.65), 3.13(40.35)	2.45	0.004	0.40

**Table S10.** The calculated vertical transition energies of IMDCS in solution at TD-DFT level of theory (PCM/CAM-B3LYP/6-31G(d,p)). Singlet oscillator strength  $f$  and CI contributions

Trans.	$\lambda$ / nm ( $f$ )	CI Description	$\lambda$ / nm ( $f$ )	CI Description	$\lambda$ / nm ( $f$ )	CI Description
		THF		DMF		DMSO
$S_0 \rightarrow S_1$	415.8 (2.28)	H $\rightarrow$ L (90.6%) H-1 $\rightarrow$ L+1 (4.6%) H-4 $\rightarrow$ L (2.9%)	415.5 (2.28)	H $\rightarrow$ L (90.6%) H-1 $\rightarrow$ L+1 (4.5%) H-4 $\rightarrow$ L (3.0%)	415.1 (2.27)	H $\rightarrow$ L (90.6%) H-1 $\rightarrow$ L+1 (4.5%) H-4 $\rightarrow$ L (3.0%)
$S_0 \rightarrow S_2$	324.9 (0.00)	H-1 $\rightarrow$ L (82.2%) H $\rightarrow$ L+1 (10.8%) H-3 $\rightarrow$ L (2.9%)	324.1 (0.00)	H-1 $\rightarrow$ L (82.0%) H $\rightarrow$ L+1 (11.0%) H-3 $\rightarrow$ L (2.8%)	323.8 (0.00)	H-1 $\rightarrow$ L (82.1%) H $\rightarrow$ L+1 (10.9%) H-3 $\rightarrow$ L (2.8%)
$S_0 \rightarrow S_3$	301.1 (0.00)	H-3 $\rightarrow$ L (80.4%) H-2 $\rightarrow$ L+1 (11.5%) H-1 $\rightarrow$ L (4.03%)	299.8 (0.00)	H-3 $\rightarrow$ L (80.7%) H-2 $\rightarrow$ L+1 (11.4%) H-1 $\rightarrow$ L (3.9%)	299.7 (0.00)	H-3 $\rightarrow$ L (80.7%) H-2 $\rightarrow$ L+1 (11.4%) H-1 $\rightarrow$ L (3.9%)
$S_0 \rightarrow S_4$	301.0 (0.04)	H-2 $\rightarrow$ L (84.3%) H-3 $\rightarrow$ L+1 (11.1%)	299.8 (0.03 76)	H-2 $\rightarrow$ L (84.4%) H-3 $\rightarrow$ L+1 (11.1%)	299.7 (0.04)	H-2 $\rightarrow$ L (84.4%) H-3 $\rightarrow$ L+1 (11.1%)
$S_1 \rightarrow S_0$	532.8 (2.46)	H $\rightarrow$ L (94%) H-1 $\rightarrow$ L-1 (3.0%)	545.5 (2.48)	H $\rightarrow$ L (94%) H-1 $\rightarrow$ L-1 (3.0%)	546.1 (2.48)	H $\rightarrow$ L (94%) H-1 $\rightarrow$ L-1 (3.0%)



### 3. QM:MM Calculations

Geometry optimization and vertical transition energies were calculated at a hybrid QM:MM approach, where the QM layer comprised of IMDCS dimers with the interacting DMSO molecules embedded in an MM molecular shell of 1 nm built according to the crystal structure and treated with the Dreiding force field. The atoms in the MM layer were frozen and optimization was carried out only to the QM layer with 6-31G (d,p) basis set with B3LYP-GD3BJ dispersion corrected functional. CAM-B3LYP functional which is the long-range corrected version of B3LYP using the Coulomb-attenuating method has been reported to better simulate the vertical transition energies has been employed with the same basis set for calculating the vertical transition energies for ground and excited states.

**Table S11.** The vertical transition energies of IMDCS in Y-form, calculated at TD-DFT level of theory (CAM-B3LYP/6-31G(d,p)) with an dispersion correction function of GD3BJ.

Transition	E /eV	E /nm	<i>f</i>	CI Description
S <sub>0</sub> →S <sub>1</sub>	2.922	424.26	0.0001	H→L (64.01%), H-1→L+1 (23.98%), H-3→L (2.94%), H-8→L (2.23%)
S <sub>0</sub> →S <sub>2</sub>	3.174	390.59	3.5089	H→L+1 (51.69%), H-1→L (38.12%), H-2→L+1 (3.48%)
S <sub>0</sub> →S <sub>3</sub>	3.2807	377.92	0.0294	H-1→L (48.69 %), H→L+1 (28.04%), H-2→L (17.15%), H-3→L+1 (2.05%)
S <sub>0</sub> →S <sub>4</sub>	3.3334	371.94	0.0001	H-1→L+1 (59.89%), H→L (20.56%), H-2→L+1(12.10%), H-3→L (2.47%)
S <sub>1</sub> →S <sub>0</sub>	2.5686	482.70	0.0086	H→L (85.66%), H-1→L+1 (5.60%), H-3→L (2.51%)